J. Phys. Chem. A **2002,** *106,* 9502−9505

Kinetic Analysis and Solvent Effects in the Carbonylation of $RuCl_3{\cdot}3H_2O$

Rina Tannenbaum

School of Materials Science and Engineering, Georgia Institute of Technology, Atlanta, Georgia 30332-0245

Received: May 26, 2002; In Final Form: July 23, 2002

The carbonylation of $RuCl_3{\cdot}3H_2O$ in refluxing alcohol represents the entry point to ruthenium organometallic chemistry. The overall carbonylation reaction is composed of three consecutive reactions, each step resulting in a ruthenium carbonyl complex with different Ru/CO ratios. A kinetic analysis of the overall reaction reveals the parameters that are involved in the rates of formation of each compound, and as a result, provides a method for the control of product composition.

1. Introduction

The carbonylation of $RuCl_3{\cdot}3H_2O$ represents the first step in the formation of ruthenium precursors and an "entry" point to ruthenium organometallic synthesis.[1] It has been observed[2−6] that the carbonylation occurs as a stepwise process having three distinct ruthenium carbonyl species as intermediates. The sequential steps of this carbonylation reaction have been discussed in a previous publication,[6] and are shown below in eq 1:

$$\left\{\begin{array}{l} \underset{\mathbf{X}}{RuCl_3{\cdot}3H_2O} \xrightarrow{\mathbf{k_1},CO,EtOH} RuCl_2(CO)(EtOH)_3 + EtCl \\ \underset{\mathbf{Y}}{RuCl_2(CO)(EtOH)_3} \xrightarrow{\mathbf{k_2},CO,EtOH} RuCl_2(CO)_2(EtOH)_2 \\ \underset{\mathbf{Z}}{RuCl_2(CO)_2(EtOH)_2} \xrightarrow{\mathbf{k_3},CO,EtOH} \underset{\mathbf{W}}{RuCl_2(CO)_3(EtOH)} \end{array}\right. \qquad (1)$$

The predominant presence of compound ***Z*** is indicated by the "wine-red" color of the solution, while the predominant presence of compound ***W*** is characterized by the "lemon-yellow" color of the solution.[6] When each of these intermediates is isolated and used as the reactant in the same organometallic substitution reactions, either different ruthenium complexes are formed,[7] or the same complex is formed via different mechanisms.[8] Since Ru(II) is a six-coordinate d^6 center, there are different numbers of alcohol molecules coordinated to the carbonyl complex, depending on the number of available coordination sites. The addition of CO ligands during the carbonylation process involves the displacement of alcohol molecules and the preferential coordination of the CO groups in their place, according to the following general substitution scheme:

$$RuCl_2(CO)_x(ROH)_{4-x} \xrightarrow{CO} RuCl_2(CO)_{x+1}(ROH)_{4-(x+1)} \qquad (2)$$

The size of the alcohol molecules used as a solvent is expected to have a significant effect on the rates of the consecutive reactions, and hence, on the relative concentrations of the various intermediates in the reaction mixture.[9−14] Therefore, it is very important to analyze the kinetics of this reaction and assess qualitatively, and if possible, quantitatively, the appropriate conditions necessary for the preferential formation of any of these intermediates.

2. Experimental Section

One gram of $RuCl_3{\cdot}3H_2O$ (purchased from Aldrich Chemicals and used without recrystallization) was dissolved in 30 mL of ethanol (purchased from Fluka and dried on a molecular sieve and redistilled before use). The solution was placed in a three-neck, 100 mL round-bottom flask equipped with a reflux setup on one neck, a bubbler on another neck, and a rubber stopper on the third neck. The reflux column was connected to an outlet, which was connected in turn to a gas buret filled with dilute $CuSO_4$. This was used to monitor the rate of bubbling, by observing the total volume displaced by the gas as a function of time. The reaction apparatus was first flushed with Ar, and the reaction was conducted at 78 °C under CO bubbling. All infrared spectra were recorded on a Perkin-Elmer 467B grating infrared spectrophotometer using a liquid demountable cell with 0.01 cm spacers and CaF_2 windows. The spectra were digitalized using UN-SCAN-IT software. The decrease in the concentration of $RuCl_3{\cdot}3H_2O$ was monitored with a Perkin-Elmer 552 UV−Vis spectrophotometer at the analytical bands of 359 and 493 nm.

3. Results and Discussion

3.1. Development of a Kinetic Model. The consecutive reactions can be modeled according to the kinetic rate expressions given in eq 3:

$$\left\{\begin{array}{l} -\dfrac{dX}{dt} = k_1 X[CO][EtOH]^3 \Rightarrow k_1[CO][EtOH]^3 = \mathbf{k'_1} \\ -\dfrac{dY}{dt} = -\mathbf{k'_1} X + k_2 Y[CO] \Rightarrow k_2[CO] = \mathbf{k'_2} \\ -\dfrac{dZ}{dt} = -\mathbf{k'_2} Y + k_3 Z[CO] \Rightarrow k_3[CO] = \mathbf{k'_3} \\ \dfrac{dW}{dt} = -\mathbf{k'_3} Z \end{array}\right. \qquad (3)$$

All reactions are performed in excess ethanol or 2-methoxyethanol (initial dilute solutions of $RuCl_3{\cdot}3H_2O$), and since the rate of CO bubbling through the solution is maintained constant in each reaction trial, the individual rate coefficients can be redefined by assuming constant concentrations of alcohol solvent and carbon monoxide. The changes in the concentrations of all four main species may be obtained experimentally via the signature UV−Vis and infrared absorption bands of the ruthenium precursor and ruthenium carbonyl ligands.[6] Moreover, since the observed kinetics is first order with respect to reactant concentration, the intensity of the infrared carbonyl absorption

10.1021/jp026187t CCC: $22.00 © 2002 American Chemical Society
Published on Web 09/14/2002

bands (which are linearly proportional to the carbonyl ligand concentration) can be used directly in the kinetic expressions.

Normalization of the variables to obtain dimensionless coefficients uses the following definitions:

$$\tau \equiv k_1' t,\ \gamma_2 \equiv \frac{k_2'}{k_1'},\ \gamma_3 = \frac{k_3'}{k_1'},\ a_i \equiv \frac{[A_i]}{[A_{x,0}]} \qquad (4)$$

Therefore, the concentrations of the four compounds are calculated according to the following relationships in the set of expressions summarized in eq 5:

$$\begin{cases} X = a_i e^{-\tau} \\ Y = \dfrac{a_i}{\gamma_2 - 1}(e^{-\tau} - e^{-\gamma_2 \tau}) \\ Z = \dfrac{a_i \gamma_2}{(\gamma_2 - 1)(\gamma_3 - 1)(\gamma_3 - \gamma_2)}[(\gamma_3 - \gamma_2)e^{-\tau} - \\ \qquad (\gamma_3 - 1)e^{-\gamma_2 \tau} + (\gamma_2 - 1)e^{-\gamma_3 \tau}] \end{cases} \qquad (5)$$

We then examined the behavior of the system of equations under various conditions. We have chosen three sets of conditions: (1) The rates of formation of both the "red" and "yellow" solutions are similar, i.e., $\gamma_2 \approx \gamma_3$; (2) The rate of formation of the "red" solution is larger than that of the "yellow" solution, and hence the predominant compound is the compound ***Z***, i.e., $\gamma_2 \gg \gamma_3$; (3) The rate of formation of the "yellow" solution is larger than that of the "red" solution, and hence the predominant compound is the compound ***W***, i.e., $\gamma_2 \ll \gamma_3$. Figure 1a shows the kinetic behavior of the four ruthenium components for the case where $\gamma_2 \approx \gamma_3$. Under these conditions, the rate of carbonylation of $RuCl_3{\cdot}3H_2O$ allows for the formation of compound ***Y*** and subsequently, a noticeable amount of the "red" solution. Only upon continuous bubbling of CO, does the concentration of the "red" solution in the mixture decrease and the final product, the "yellow" solution, becomes the dominant component.

Figure 1b shows the kinetic behavior of the four ruthenium components for the case where $\gamma_2 \gg \gamma_3$. Under these conditions, the rate of carbonylation of $RuCl_3{\cdot}3H_2O$ allows for the formation of compound ***Y*** for a short time, and subsequently, a noticeable amount of the "red" solution. Despite continuous bubbling of CO, the formation of compound ***W*** is suppressed even at larger values of τ, and the concentration of the "red" solution in the mixture dominates for the time window used for experimentation. Eventually, after $\tau > 20$, the "yellow" solution starts to form. Indeed, if the experimental time is allowed to reach $\tau \rightarrow \infty$, the "yellow" solution will dominate the mixture.

Figure 1c shows the kinetic behavior of the four ruthenium components for the case where $\gamma_2 \ll \gamma_3$. Under these conditions, the rate of carbonylation of $RuCl_3{\cdot}3H_2O$ allows for the formation of compound ***Y*** for a short time, and subsequently, the formation of the "yellow" solution with only a small amount of the "red" solution. In this case the formation of compound ***Z*** is completely suppressed. It is interesting to note that compound ***Y***, the intermediate ruthenium carbonyl compound, is always formed at low τ, $\tau < 5$, at constant maximal concentration. This is due to the fact that we have explored the behavior of the system by keeping γ_2 constant and varying γ_3, effectively changing the ratio between the two, and hence, since ***Y*** is a function of τ and $\gamma_2{\cdot}\tau$, its concentration will be identical in all three situations.

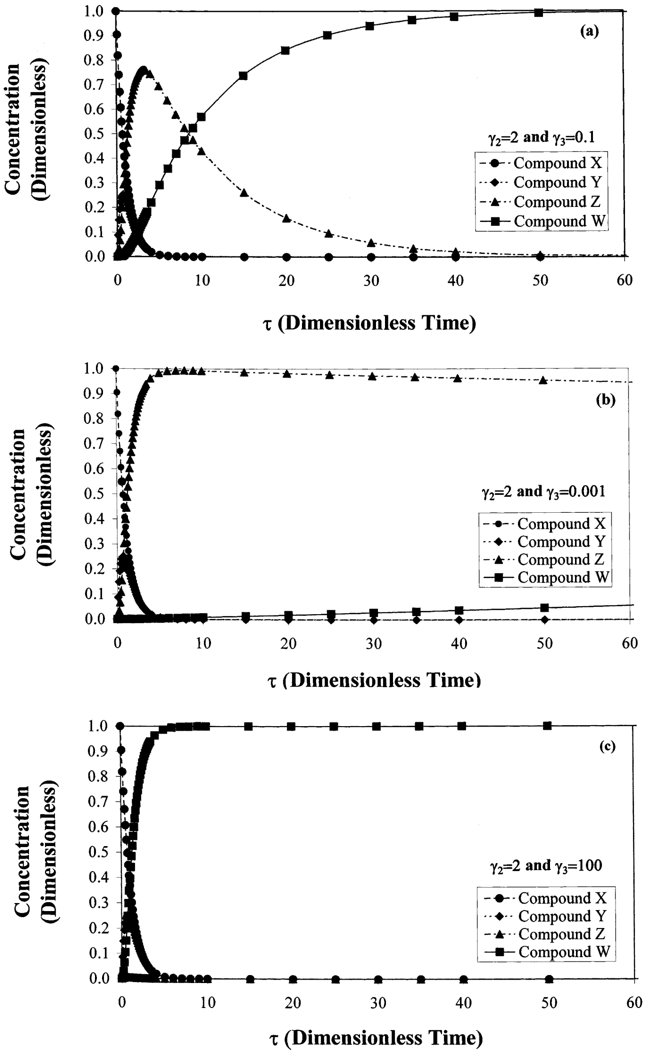

Figure 1. (a) The kinetic behavior of the four ruthenium components for the case where $\gamma_2 \approx \gamma_3$, i.e., specifically, $\gamma_2 = 2$ and $\gamma_3 = 0.1$. (b) The kinetic behavior of the four ruthenium components for the case where $\gamma_2 \gg \gamma_3$, i.e., specifically, $\gamma_2 = 2$ and $\gamma_3 = 0.001$. (c) The kinetic behavior of the four ruthenium components for the case where $\gamma_2 \ll \gamma_3$, i.e., specifically, $\gamma_2 = 2$ and $\gamma_3 = 100$.

3.2. Analysis of Experimental Data. Figure 2 shows the progression of the infrared spectra as a function of time while bubbling CO through the ruthenium solution to maintain a constant CO concentration in the solution. The infrared spectrum of the initial carbonyl mixture, of which compound ***Y*** is the dominant species, is characterized by absorption peaks at 1951, 1974, 1993, 2045, and 2068 cm^{-1} that appear immediately upon the start of the carbonylation process. With continuous CO bubbling through the solution, the solution becomes red (compound ***Z***), and the following changes in the spectrum occur: the 1974 and 2045 cm^{-1} bands disappear, while the 1993 and 2068 cm^{-1} bands increase in intensity and become the dominant absorption bands of the spectrum.[15,16] The main conclusion for this step is that the 1974 and 2045 cm^{-1} bands belong exclusively to compound ***Y***, while the other bands observed in the initial spectrum overlap with those of the subsequent compound ***Z***. The two infrared bands for this compound indicate that the only CO group can assume two different positions: the higher energy band is due to a ruthenium compound with a higher symmetry, in which the CO group is in the equatorial position with the two Cl atoms in the trans-axial positions, and the lower energy band is due to a CO group in the axial position, with one equatorial and one axial Cl atoms. When CO is further bubbled through the "red solution",

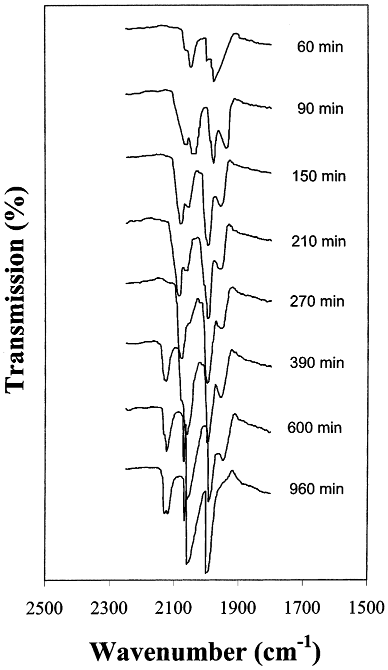

Figure 2. Stacking of the infrared spectra of the carbonylation reaction of $RuCl_3 \cdot 3H_2O$ in ethanol. The progression of the spectra is from top to bottom. The spectra are shown in % transmission, but due to the stacking option, the actual values have been removed.

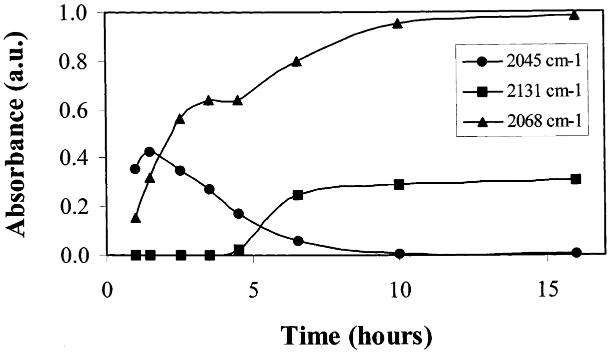

Figure 3. Plot of the absorbances of the three analytical bands 2045, 2068, and 2131 cm^{-1} as a function of time, during constant bubbling of CO through the ruthenium solution.

compound ***Z***, the 2045 cm^{-1} remaining shoulder disappears and a new band at 2131 cm^{-1} appears. The resulting "yellow solution", compound ***W***, is characterized by the presence of the 1951, 1993, 2068, and 2131 cm^{-1} absorption bands. Hence, a complete disappearance of the 2045 cm^{-1} band indicates the pseudo-equilibrium formation of compound ***Z***, and the appearance of the 2131 cm^{-1} band indicates the formation of compound ***W***. A plot of the relevant and analytically useful 2045, 2068, and 2131 cm^{-1} absorption bands as a function of time is shown in Figure 3.[6] Since it is clear that compound ***Y*** is characterized by the 1974 and 2045 cm^{-1} bands, the initial increase in the 2068 cm^{-1} band is due mainly to the formation of compound ***Z***. Therefore, the initial increase in the intensity of these three bands may be used to estimate independently the initial rate coefficients for the formation of compounds ***Y***, ***Z***, and ***W***. From the rate coefficients it is possible to calculate the values of τ, γ_2, and γ_3 shown in Table 1. Once these experimental values were obtained, they were introduced into eq 5, and solved simultaneously, to obtain the experimental concentration profile for all the four species involved in these consecutive reactions, as shown in Figure 4. Note that the concentration of the ruthenium carbonyl species is shown in actual concentration units and not as mole fractions.

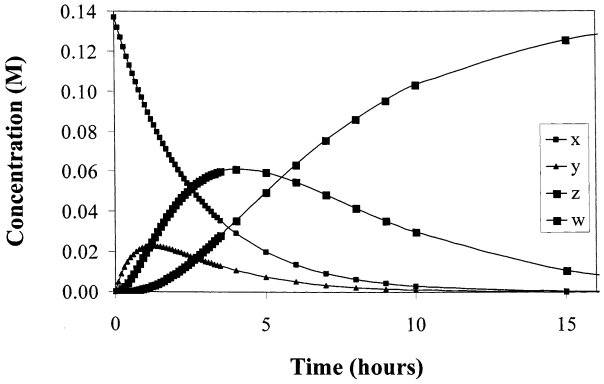

Figure 4. The calculated concentration profile for all the four ruthenium species involved in these consecutive reactions using the experimental values of the rate constants $\gamma_2 = 3.69$ and $\gamma_3 = 0.61$, obtained from the infrared spectra of the process.

TABLE 1: The Specific Experimental Rate Coefficients Used for the Calculation of the Concentrations of the Four Ruthenium Intermediates during the Carbonylation Reaction

τ	γ_2	γ_3
$1.07 \times 10^{-4} (s^{-1}) \cdot t$ (s)	3.69	0.61

TABLE 2: Calculated Molar Extinction Coefficients of the Three Ruthenium Carbonyl Complexes for the 2045, 2068, and 2131 cm^{-1} Infrared Bands

analytical IR band (cm^{-1})	ϵ_Y ($L\ mol^{-1}\ cm^{-1}$)	ϵ_Z ($L\ mol^{-1}\ cm^{-1}$)	ϵ_W ($L\ mol^{-1}\ cm^{-1}$)
2045	1380.64		
2068	1466.65	56.37	718.25
2131			224.09

The direct correlation between the infrared data and the calculated concentration profiles of the various ruthenium intermediates in the solution yielded a useful method for the calculation of the molar absorption extinction coefficients of the three main carbonyl species at different spectral frequencies. The 2045 cm^{-1} band is specific to $RuCl_2(CO)(EtOH)_3$ (***Y***), and the 2131 cm^{-1} band is specific to $RuCl_2(CO)_3(EtOH)$ (***W***). At $t = 0$, the 2068 cm^{-1} band may belong to both compounds ***Y*** and ***Z***, and at $t = \infty$ it belongs exclusively to $RuCl_2(CO)_3(EtOH)$ (***W***). At any time $0 < t < \infty$, this analytical band is the result of the mixture of all three carbonyl-containing ruthenium complexes in solution. Therefore, it is possible to express the intensities of this band at three different times, A_{t_1}, $A_{t_2,}$ and A_{t_3}, extracted from the infrared data in Figure 3, as a function of the corresponding concentrations of the three components, extracted from the concentration calculations in Figure 4. By solving this set of three equations, we were able to calculate the individual molar extinction coefficients at 2068 cm^{-1} for each of the three ruthenium carbonyl components, ϵ_Y, ϵ_Z, and ϵ_W, as summarized in Table 2. The results indicate that the intensity of the 2068 cm^{-1} band is dominated by the presence of compounds ***Y*** and ***W***, and compound ***Z*** contributes to the intensity of this band only when it is present in relatively large amounts. Hence, at the onset of the reaction, when compound ***Y*** begins to decrease and compound ***W*** has not yet been formed ($t = \sim 60$ min), the initial increase in the 2068 cm^{-1} band can indeed be attributed to the increase in the concentration of compound ***Z***.

3.3. Effect of the Size of the Solvent Molecule. When the carbonylation of $RuCl_3 \cdot 3H_2O$ is conducted in 2-methoxyethanol instead of ethanol, only a "yellow" solution is formed, without

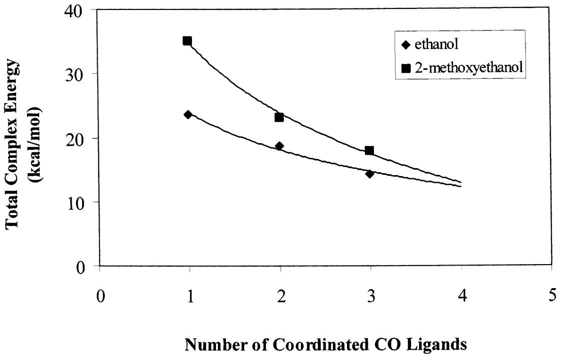

Figure 5. Plot of the changes in the total energies of the ruthenium complexes involved in the carbonylation reaction, in the presence of both ethanol and 2-methoxyethanol, as a function of the number of CO groups coordinated to the central Ru metal. The total energies were calculated with Gaussian 98 software.

TABLE 3: Total Energies of the Various Ruthenium Carbonyl Complexes Present during the Carbonylation Reaction, in the Presence of Ethanol or 2-Methoxyethanol

intermediate compounds	total energy (kcal/mol)
$RuCl_2(CO)(ethanol)_3$ (***Y***)	23.7
$RuCl_2(CO)(2\text{-methoxyethanol})_3$ (***Y′***)	35.2
$RuCl_2(CO)_2(ethanol)_2$ (***Z***)	18.7
$RuCl_2(CO)_2(2\text{-methoxyethanol})_2$ (***Z′***)	23.1
$RuCl_2(CO)_3(ethanol)$ (***W***)	14.3
$RuCl_2(CO)_3(2\text{-methoxyethanol})$ (***W′***)	18.0
$RuCl_2(CO)_4$ (theoretical complex used as standard)	12.7

a "red" solution as intermediate.[6−8] The reactions in both solvents are compared in eq 6:

$$RuCl_3{\cdot}3H_2O \xrightarrow{\text{ethanol reflux} \approx 4\text{ h}, \approx 80\ ^\circ\text{C}} \text{“red” solution}$$

$$RuCl_3{\cdot}3H_2O \xrightarrow[\text{reflux} \approx 6\text{h}, \approx 125\ ^\circ\text{C}]{\text{2-methoxyethanol}} \text{“yellow” solution} \qquad (6)$$

In both cases, the first step in the reaction is the formation of a complex with one CO ligand bound to the central Ru atom, and the three alcohol molecules coordinated through the three available coordination sites of the metal (complex ***Y*** in the case of ethanol). Comparison of the energies of both complexes (using energy minimization software Gaussian 98), reveals that the coordination of the 2-methoxyethanol molecules to the ruthenium center destabilizes the complex due to the introduction of large steric effects,[17] which were less notable in the case of ethanol. Hence, the formation of the complex $RuCl_2(CO)$-$(2\text{-methoxyethanol})_3$ is highly unfavored, as evidenced by the total energy of the complexes formed, shown in Table 3, and so, once it is formed it immediately reacts. The same argument may be also made for the subsequent intermediate, the complex equivalent to complex ***Z*** for the ethanol case. The net result of this process is the formation of the tri-carbonyl ruthenium complex with only one coordinated 2-methoxyethanol molecule, equivalent to complex ***W*** for the ethanol case. Figure 5 shows the changes in the total energies of the ruthenium complexes with both ethanol and 2-methoxyethanol as a function of the number of CO groups coordinated to the central metal. Since a higher number of CO groups implies a lower number of solvent molecules coordinated to the metal, the steric effect becomes less important, and the overall energies of the complexes decrease. The trend was extended to a theoretical situation of four CO groups, i.e., no coordinated solvent molecules, and indeed the energies intersect. Figure 6 shows a comparison between the absorption of the 2131 cm^{-1} band for the ethanol case and the 2-methoxyethanol case. As expected from the stability arguments presented earlier, the rate of formation of the "yellow" solution in the presence of 2-methoxyethanol is at least 2-fold larger than that observed in the presence of ethanol. The detailed rate analysis is shown in Table 4. The molar extinction coefficients for the analytical infrared bands of the complex that were previously calculated were used to determine the concentration of the three different carbonyl species in the mixture. The effective rate coefficient for the formation of the di-carbonyl complex was found to be negligible, and hence, γ_2 in this case was approximated to be equal to zero. In this case, therefore, $\gamma_2 < \gamma_3$ (as with the reaction conditions shown in Figure 1c), and the reaction proceeded directly to form the "yellow" solution.

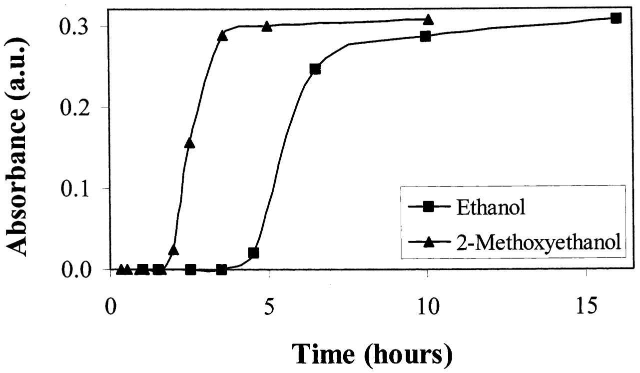

Figure 6. A comparison between the absorption of the 2131 cm^{-1} infrared band for the formation of $RuCl_2(CO)_3(ROH)$ for the ethanol case and the 2-methoxyethanol case.

TABLE 4: Experimental Values for the Various Rate Constants of the Carbonylation Reaction in the Presence of Ethanol or 2-Methoxyethanol

solvent	k_1 (s^{-1})	k_2 (s^{-1})	k_3 (s^{-1})	γ_2	γ_3
ethanol	1.07×10^{-4}	3.94×10^{-4}	6.48×10^{-5}	3.69	0.61
2-methoxyethanol	4.09×10^{-5}	∼0	8.67×10^{-5}	∼0	2.12

Acknowledgment. The author is indebted to Dr. Emmanuel Tannenbaum for his help with Mathematica, and Ms. Marcela Anghelovitz for her help with the raw calculations based on the infrared spectra.

References and Notes

(1) Chatt, J.; Shaw, B. L.; Field, A. E. *J. Chem. Soc.* **1964**, 3466.
(2) Stevenson, T. A.; Wilkinson, G. *J. Inorg. Nucl. Chem.* **1966**, *28*, 945.
(3) Daives, T. L.; Holmes, T. D. *Inorg. Nucl. Chem. Lett.* **1971**, *7*, 847.
(4) Mantovani, A.; Cenini, S. *Inorg. Synth.* **1976**, *16*, 45.
(5) Berch, M. L.; Davison, A. *J. Inorg. Nucl. Chem.* **1973**, *35*, 3763.
(6) Tannenbaum, R. *Inorg. Chim. Acta* **1987**, *130*, 49.
(7) Tannenbaum, R. *Inorg. Chim. Acta* **1988**, *148*, 199.
(8) Tannenbaum, R. *Chem. Mater.* **1994**, *6*, 550−555.
(9) Angelici, R. J.; Basolo, F. *Inorg. Chem.* **1963**, *2*, 728.
(10) Poë, A. J.; Twigg, M. V. *Inorg. Chem.* **1974**, *13*, 2982.
(11) Johnson, B. F. G.; Lewis, J.; Twigg, M. V. *J. Chem. Soc., Dalton Trans.* **1975**, 1876.
(12) Howell, J. A. S.; Burkinshaw, P. M. *Chem. Rev.* **1983**, *83*, 557.
(13) Chen, L.; Poë, A. J. *Inorg. Chem.* **1989**, *28*, 3641.
(14) Basolo, F. *Polyhedron* **1990**, *9*, 1503.
(15) Darensbourgh, D. J.; Nelson, H. H.; Hyde, C. L. *Inorg. Chem.* **1974**, *9*, 2135.
(16) Dierkes, P.; Van Leeuwen, P. W. N. M. *J. Chem. Soc., Dalton Trans.* **1999**, 1519.
(17) Bunten, K. A.; Farrar, D. H.; Poë, A. J.; Lough, A. J. *Organometallics* **2000**, *19* (18), 3674−3682.